AJNR Am J Neuroradiol 23:1121–1127, August 2002

Aneurysms of the Anterior Communicating Artery Treated with Guglielmi Detachable Coils: Follow-Up with Contrast-Enhanced MR Angiography

Xavier Leclerc, Jean-François Navez, Jean-Yves Gauvrit, Jean-Paul Lejeune, and Jean-Pierre Pruvo

BACKGROUND AND PURPOSE: **The long-term outcome of patients treated with Guglielmi detachable coils (GDCs) remains unknown and is being evaluated. We sought to assess the feasibility and utility of contrast-enhanced MR angiography in the follow-up of anterior communicating artery (AcomA) aneurysms treated with GDCs.**

METHODS: **In a prospective study, 20 consecutive patients with AcomA aneurysms underwent digital subtraction angiography (DSA), time-of-flight MR angiography (TOF-MRA), and contrast-enhanced MR angiography (MRA) 12 months after treatment with GDCs. The aneurysmal sac measured less than 10 mm in 19 patients and 12 mm in one patient. Two observers who did not analyze the DSA images independently reviewed the MRA images. Aneurysms were classified according to the presence of a residual neck (ie, complete occlusion, small residual neck, large residual neck, or not assessable). DSA was used as the standard of reference.**

RESULTS: **Images from all examinations were assessable. Venous enhancement was observed in five cases at contrast-enhanced MRA; this did not affect image interpretation. Interobserver agreement was good. A comparison of the techniques showed good agreement in the detection of a residual neck. Two cases of a small residual neck were not detected at TOF-MRA, and one case of complete occlusion was misclassified as a small residual neck at contrast-enhanced MRA.**

CONCLUSION: **Our findings showed that contrast-enhanced MRA is a valuable method for the follow-up of aneurysms in the AcomA after their treatment with GDCs. Further studies with multiple aneurysm locations and larger groups are required to determine the exact role of this technique.**

Subarachnoid hemorrhage (SAH) is the most severe complication of intracranial aneurysms. Its incidence is estimated to be 1 case per 1000 Europeans per year (1). The treatment consists of the exclusion of the malformation from the intracranial circulation to eliminate the risk of rebleeding. Before 1990, surgical clip placement was the only valuable treatment for these malformations. Since 1991, endovascular occlusion of the aneurysmal sac with Guglielmi detachable coils (GDCs) has been an alternative approach (2). The therapeutic strategy depends mainly on the morphology of the aneurysm.

The long-term outcome of patients treated with GDCs remains unknown and is being evaluated. A regrowth of the aneurysm or a remnant aneurysmal neck may be detected after treatment (3). Several imaging strategies may be used to image the residual neck. Digital subtraction angiography (DSA) remains the technique of choice, but this method is relatively invasive and poses a risk of neurologic complications. Helical CT angiography with three-dimensional (3D) reconstructions has been proven effective in the detection of small aneurysms (4), but coil-related artifacts may hinder the detection of a residual flow in the aneurysm. Time-of-flight MR angiography (TOF-MRA) is considered as an alternative approach to DSA. This method is effective in the detection of small intracranial aneurysms and in the follow-up of patients after embolization (5–12). However, the rel-

Received December 20, 2001; accepted after revision March 21, 2002.

From the Departments of Neuroradiology (X.L., J.F.N, J.Y.G., J.P.P.) and Neurosurgery (J.PL.), Salengro Hospital, University Hospital, Lille, France.

Address reprint requests to X. Leclerc, MD, Service de Neuroradiologie, Hôpital Roger Salengro, Boulevard du Professeur Leclercq, 59037 Lille Cedex, France.

atively long acquisition time and the presence of flow-related artifacts are limiting factors in TOF-MRA. To improve vascular conspicuity, some have suggested the administration of contrast medium before performance of TOF-MRA. However, because of the long acquisition time, venous enhancement often degrades the image quality (8, 13).

Important advances in MR angiography (MRA) have been made recently. Ultrafast contrast-enhanced MRA is based on the T1-shortening effect of moving spins, which minimizes the saturation effect of slow flow without major venous enhancement. Such sequences are effective in the evaluation of carotid stenoses (14), and recent findings in the evaluation of intracranial aneurysms are promising (15, 16). However, to our knowledge, this method has not been evaluated in the visualization of intracranial vasculature after GDC treatment.

The aim of the present study was to follow up a group of patients with ruptured aneurysms of the anterior communicating artery (AcomA) that were treated with GDCs. Our purpose was to assess the reliability of contrast-enhanced MRA in the detection of a residual neck. Findings were compared with those of DSA, as the reference technique, and to those of TOF-MRA, which is widely used in routine evaluation of SAH.

Methods

Study Design

To evaluate the feasibility of contrast-enhanced MRA in the detection of aneurysm repermeation after embolization, we performed both MRA and DSA at 12-month follow-up in consecutive patients treated with GDCs for a ruptured aneurysm of the AcomA. All patients in the present study were referred from the neurosurgery department. The indication of treatment depended on the clinical condition of the patient, the location of the aneurysm, the size of the aneurysmal sac, and the size of the aneurysmal neck. In our institution, if DSA depicts an aneurysm of the AcomA with a diameter less than 10 mm and a small neck, the patient is referred to the neuroradiology department for potential endovascular treatment with GDCs. After treatment, both MRA and DSA are planned at 12 months, according to a protocol approved by our institutional review board. Both examinations are performed within 48 hours of each other in all patients. MR examinations include both 3D-TOF and gadolinium-enhanced fast 3D angiographic sequences. DSA is considered the reference standard.

Patients

This study included 20 patients (nine women,11 men; median age, 49 years; age range, 17 –73 years) who were admitted between November 1996 and December 1999 for a ruptured aneurysm of the AcomA. In all cases, CT performed on an emergency basis showed a diffuse SAH located mainly at the anterior interhemispheric sulcus. In two patients, the bleeding was associated with a frontal hematoma. DSA performed the day after admission showed a saccular aneurysm of the AcomA; the maximal diameter of the aneurysmal sac was less than 5 mm in seven patients, 5–10 mm in 12 patients, and 12 mm in one patient. These patients were referred to the neuroradiology department for endovascular treatment, according to our protocol. In one case, despite a 12-mm aneurysmal sac, the patient was treated with GDCs because of the posterior orientation of the aneurysm that would have increased the risk of the neurosurgical procedure. All aneurysms were treated within 3 days after SAH by using GDCs of various diameters and lengths, according to the size and the morphology of the aneurysm. Endovascular procedures were performed after selective catheterization of the internal carotid artery by femoral approach. Treatment of the aneurysmal sac was angiographically complete in 18 patients and partial in two patients (one with a 7-mm aneurysm and one with a 12-mm aneurysm).

Digital Subtraction Angiography

All DSA examinations were performed by using a digital subtraction system (Integris V 3000; Philips Medical Systems, Best, the Netherlands). DSA before treatment included selective injection of both common carotid arteries with the acquisition of at least three intracranial views (frontal, sagittal, and anterior homolateral oblique). When necessary, additional oblique views were obtained to separate the aneurysmal sac from the surrounding vessels. Only the best views that showed the aneurysm during initial DSA were acquired at the end of the embolization and at 1-year DSA follow-up. Each angiogram was acquired at a rate of two images per second with a 512×512 matrix size and a 20-cm field of view. For each projection, an 8-mL bolus of iodinated contrast material (Iohexol; Nycomed, Princeton NJ) was injected at a rate of 6 mL/s by using a power injector. The total dose did not exceed 120 mL.

Imaging Technique

MR angiograms were obtained within 24 hours before DSA by using a 1.5-T system (Magnetom Vision; Siemens, Erlangen, Germany) with 25-mT/m maximum gradient strength. All examinations were performed with a standard head coil. Patients were positioned with a 20-gauge intravenous catheter inserted into their antecubital vein. After scout images were acquired in three planes, the following sequences were programmed. First, a 3D-TOF sequence was used in the axial plane that included both the carotid siphons and the A1 and A2 segments of the anterior cerebral arteries. A saturation band was placed above the acquisition volume to eliminate the venous signal. The parameters were as follows: 34/5.4 [TR/TE]; flip angle, 50°; field of view, 25; acquisition volume, 55 mm; and matrix, 200×512. The acquisition time was 4 minutes. Second, a contrast-enhanced MRA fast imaging steady-state precession sequence was performed in the coronal plane. The acquisition volume was placed on the sagittal scout image in an oblique direction so that the volume included the cervical carotid arteries, the carotid siphons, the A1 and A2 segments of the anterior cerebral arteries, the M1 and M2 segments of the middle cerebral arteries, the basilar artery, and the initial segment of the posterior cerebral arteries. The parameters were as follows: 6.8/2.3, flip angle, 35°; field of view, 25; and matrix, 150×512. The anteroposterior coverage was 60 mm, and the acquisition time was 40 seconds. A 100% zero-fill interpolation was performed in the section direction and fat saturation was used. A 0.2-mmol/kg bolus of gadolinium chelate (gadodiamide [Omniscan]; Nycomed) was injected at a rate of 2mL/s by the use of an MR-compatible power injector (Spectris; Medrad, Pittsburgh, PA). The circulation time of the contrast medium from the antecubital vein to the carotid arteries was estimated by the use of a test bolus before performance of 3D-MRA. Two-dimensional images (2D turbo flash sequence; 3.3/1.4, flip angle, 8°; field of view, 25; section thickness, 8 mm; matrix, 88×128) were acquired every second during 60 seconds at the level of the carotid siphons. The start of the test bolus injection coincided with the start of the sequence. The circulation time was then calculated by means of signal intensity measurements in a region of interest placed over either the carotid siphon or the basilar artery. The delay time was calculated so that the

TABLE 1: MR angiographic and DSA findings of intraaneurysmal flow at 12-month follow-up after GDC treatment

MR Angiographic Finding	DSA Finding			
	Complete Occlusion	Small Residual Neck	Large Residual Neck	Not Assessable
TOF image				
Complete occlusion	15	2	0	0
Small residual neck	0	2	0	0
Large residual neck	0	0	1	0
Not assessable	0	0	0	0
Contrast-enhanced image				
Complete occlusion	14	0	0	0
Small residual neck	1	4	0	0
Large residual neck	0	0	1	0
Not assessable	0	0	0	0

peak of arterial contrast enhancement coincided with the acquisition of the central part of k space according the following equation: delay time = test bolus transit time + 0.5 injection time − 0.35(acquisition time), where all times are in seconds. Source images of both TOF-MRA sequences and contrast-enhanced MRA sequences were reconstructed by using the maximum intensity projection (MIP) algorithm. Multiple projections were obtained every 15° over 180° in lateral and anteroposterior views.

Image Analysis

Two trained radiologists (X.L., J.F.N.) together reviewed the DSA images to detect a residual aneurysmal sac. The findings on each angiogram were then assigned one of four following categories: 0, complete occlusion; 1, small residual neck (1–3 mm); 2, large residual neck (larger than 3 mm); and 3, not assessable. Two examiners (including J.Y.G.) who were blinded to the results of DSA examined the MRA images. Interpretation of MRA images was made on the basis of the MIP images and by consensus. The following criteria were used: image contrast, artifact (metal, motion), vessel overlap, and patency of the intracranial arteries. Image contrast was graded as low when the signal intensity in the enhanced arterial lumen was only slightly higher than that in the background, moderate when the signal intensity was clearly higher, and high when the signal intensity was optimal. Artifacts and vessel overlaps were judged as minor when they did not prevent the interpretation of images and major when they degraded the image quality. Patency of the parent vessels was judged in the A1 and A2 AcomA segments. Each artery was graded as normal in cases of regular outlines or abnormal in cases of stenosis or occlusion involving the artery in whole or in part.

For the detection of a remnant neck, both blinded observers evaluated the MIP images in a fully randomized order. TOF-MRA images and contrast-enhanced MRA images were used independently. The findings were compared between observers and with those of DSA by using the following classifications: 0, complete occlusion; 1, small residual neck (1–3 mm); 2, large residual neck (larger than 3 mm); and 3, not assessable. Cases leading to a disagreement between the observers regarding the detection of a remnant neck on MRA images were reviewed by both readers to reach a consensus.

Statistical Analysis

The first step of the analysis consisted of an evaluation of the interobserver agreement for each set of MR images (ie, TOF-MRA images and contrast-enhanced MRA images); for this, we used the κ statistic. The second step consisted of a comparison of MR angiography and DSA in the detection of a residual neck; for this we used the same statistical tests. Kappa values greater than 0.6 suggested substantial agreement, and values greater than 0.8 indicated excellent agreement. P values less than .005 indicated a significant difference.

Results

Image Quality

The overall quality of TOF-MRA images was judged optimal in all patients. The image contrast of gadolinium-enhanced MRA images was judged excellent in 17 patients and moderate in three patients. Minor artifacts were observed on TOF-MRA images in five patients. These artifacts were related to the GDCs and did not interfere with image interpretation. No coil or motion artifact was seen on contrast-enhanced MRA images. Venous overlaps were present on contrast-enhanced MRA images in five cases and on TOF-MRA images in no case. Vessel overlaps were considered minor, because they did not prevent the interpretation of vessel conspicuity. Visualization of the anterior cerebral arteries was optimal in all cases. No stenosis or occlusion was depicted in the initial portion of intracranial arteries.

Interobserver Agreement

Interobserver agreement for the detection of a residual neck was judged low in the analysis of TOF MR angiograms ($\kappa = 0.13$, $P < .16$). Interobserver agreement was good and the difference was significant in the analysis of contrast-enhanced MRA images ($\kappa = 0.78$, $P < .001$). Discrepancies between both examiners were noted with TOF-MRA findings in six cases and with contrast-enhanced MRA findings in three cases. In these cases, an additional collaborative reading by both examiners was performed to reach a consensus.

Intertechnique Agreement

DSA revealed residual aneurysmal flow at 1-year follow-up in five patients, including one with a major residual flow (neck larger than 3 mm) and four with a minor residual flow in the aneurysmal sac (1–3 mm) (Table 1).

The comparison of TOF-MRA findings and contrast-enhanced MRA findings with those of DSA showed a good and significant agreement between

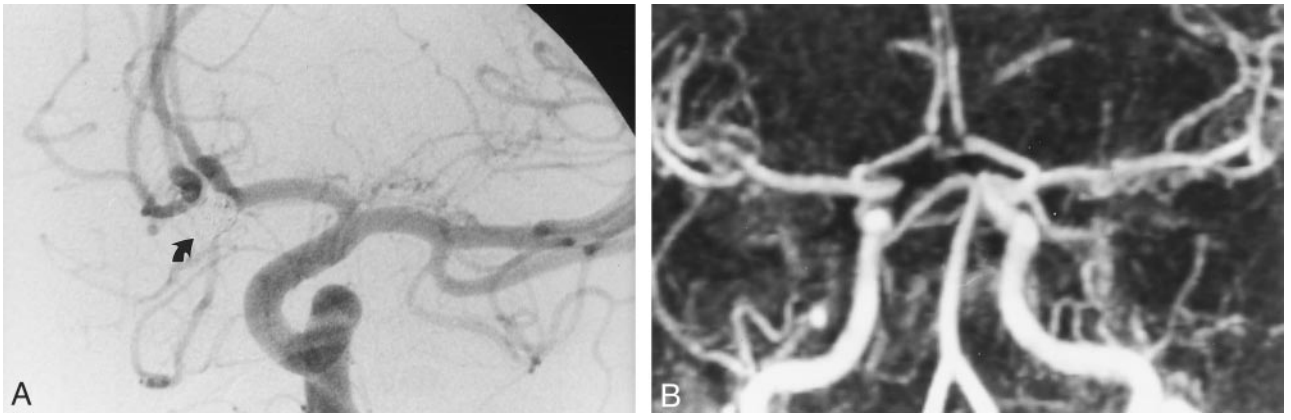

FIG 1. DSA and contrast-enhanced MRA show concordant findings.
A, Intracranial left carotid DSA obtained 12 months after the treatment of a 4-mm aneurysm in the AcomA. Frontal head view shows no remnant cavity at the site of the AcomA (*arrow*).
B, Contrast-enhanced MRA image with MIP reconstruction in the frontal view shows findings in agreement with those at DSA.

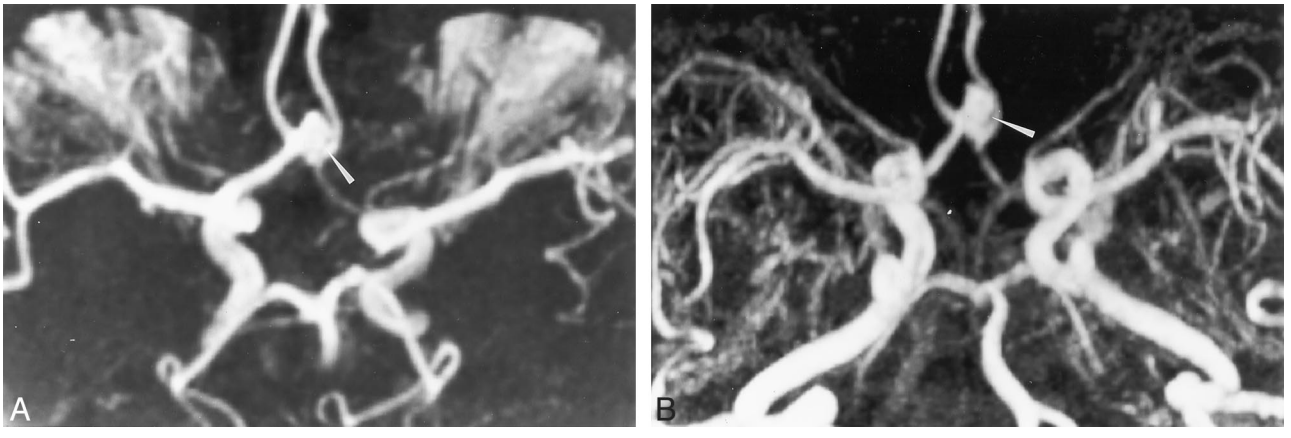

FIG 2. TOF-MRA and contrast-enhanced MRA show concordant findings.
A, TOF-MRA image obtained with MIP reconstruction obtained 12 months after the treatment of a 8-mm aneurysm in the AcomA. Axial image depicts a residual neck of 4-mm diameter (*arrowhead*).
B, Contrast-enhanced MRA image obtained with axial MIP reconstruction in the axial plane depicts a residual cavity (*arrow*), in agreement with the TOF-MRA findings.

techniques (TOF-MRA: $\kappa = 0.83, P < .001$; contrast-enhanced MRA: $\kappa = 0.73, P < .001$) (Figs 1 and 2).

Among the five cases with a residual neck at conventional angiography, TOF-MRA enabled the detection of the remnant neck in three patients. Two minor remnant necks were not detected at TOF-MRA, whereas all residual necks detected at DSA were seen at contrast-enhanced MRA (Fig 3). However, one case of complete aneurysmal occlusion, as depicted at DSA, was misclassified as a small residual neck at contrast-enhanced MRA (Fig 4). The sensitivity of MRA in the detection of a residual neck at 1-year follow-up was higher with the use of contrast-enhanced MR angiographic sequences compared with that of TOF-MRA, but its specificity was lower (Table 2).

Discussion

Our findings showed the potential utility of contrast-enhanced MRA in the follow-up of patients after GDC treatment for a ruptured intracranial aneurysm of the AcomA. A regrowth of the aneurysm or a remnant neck that was angiographically proven at 12-month follow-up was detected with a good sensitivity and with an appropriate image quality at TOF-MRA and contrast-enhanced MRA. However, TOF-MRA appeared to be less sensitive; two cases with a residual neck were not detected.

Preliminary studies have been performed to assess the usefulness of TOF-MRA for the follow-up of patients treated with GDCs for an intracranial aneurysm. In a study of 26 patients, Derdeyn et al (9) reported a sensitivity of 71% and a specificity of 89% in the detection of a residual intraaneurysmal flow. Three false-negative findings and two false-positive findings were reported in this study. These results were explained by 1) the presence of a slow flow in the aneurysm that led to the misinterpretation of a hypointense finding as a complete occlusion and 2) a residual hemorrhage that led to the misinterpretation of a hyperintense finding as residual flow. The authors suggest the use of a short TE to minimize the intravoxel spin-dephasing artifacts, the use of higher spatial resolution to improve the image quality, and the injection of contrast material to prevent satura-

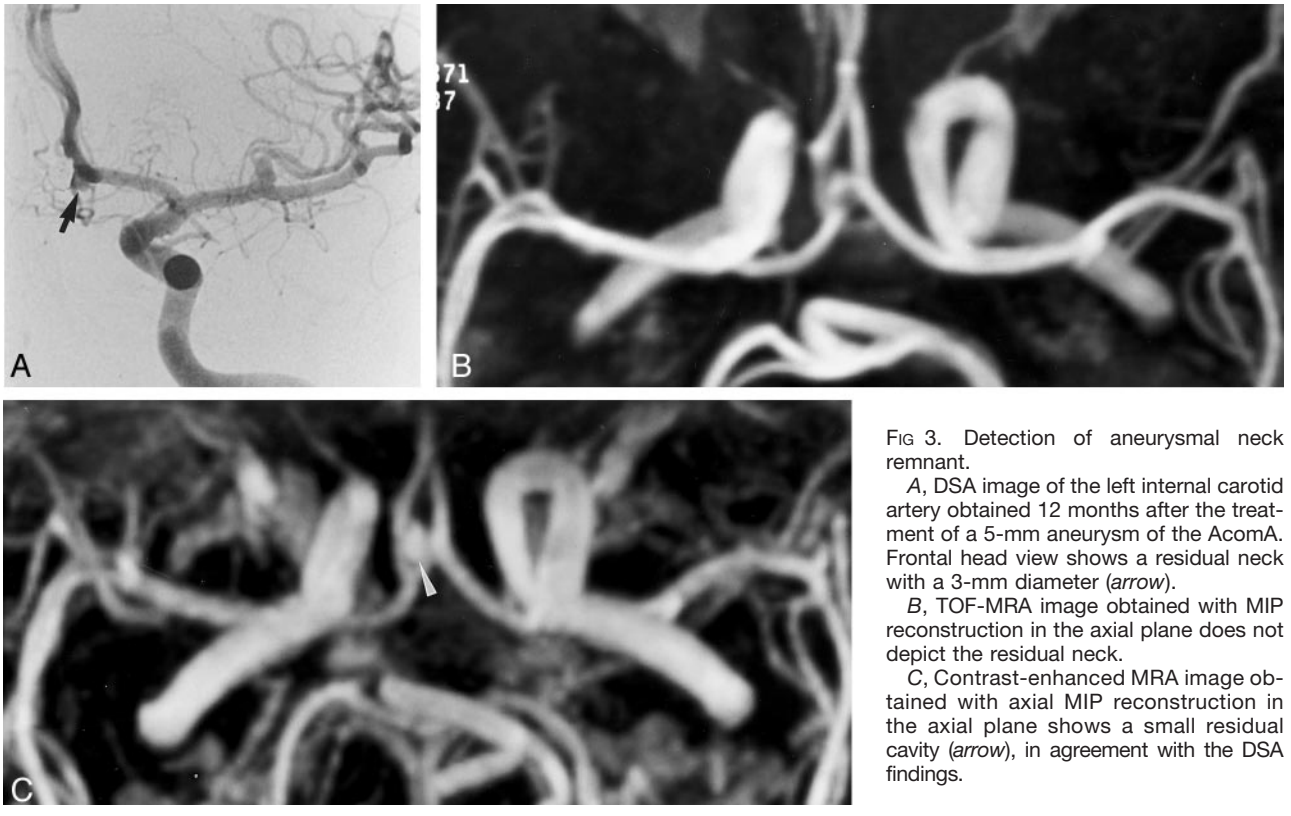

FIG 3. Detection of aneurysmal neck remnant.

A, DSA image of the left internal carotid artery obtained 12 months after the treatment of a 5-mm aneurysm of the AcomA. Frontal head view shows a residual neck with a 3-mm diameter (*arrow*).

B, TOF-MRA image obtained with MIP reconstruction in the axial plane does not depict the residual neck.

C, Contrast-enhanced MRA image obtained with axial MIP reconstruction in the axial plane shows a small residual cavity (*arrow*), in agreement with the DSA findings.

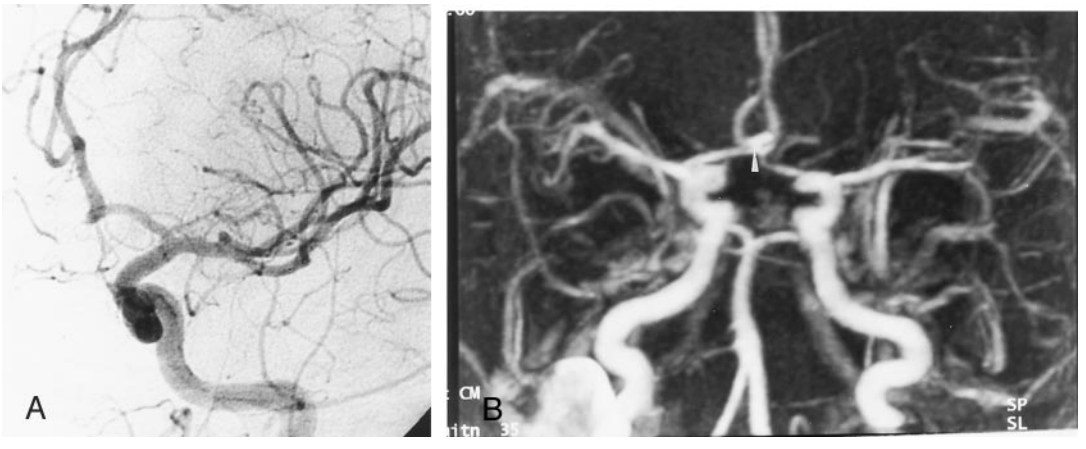

FIG 4. Patient with a 6-mm aneurysm of the AcomA that was treated with GDCs. Only the left carotid angiogram showed the aneurysm at initial DSA.

A, Left carotid artery angiogram obtained 12 months after treatment. Frontal head view shows no recurrent aneurysm.

B, Contrast-enhanced MRA image obtained with MIP reconstruction shows a hyperintense area (*arrowhead*) at the site of the AcomA. This finding was misinterpreted as a residual aneurysmal neck.

TABLE 2: Sensitivity and specificity of MR angiography and DSA in the detection of a residual aneurysmal neck at 1-year follow-up after GDC treatment

MR Angiography	Sensitivity, %	Specificity, %	Interobserver *P* Value	Intertechnique *P* Value
TOF	60	100	.16	<.001
Contrast-enhanced	100	93	<.001	<.001

tion effects. In study of patients in whom 64 intracranial aneurysms were occluded with GDCs, Anzalone et al (12) reported promising results. All residual aneurysmal sacs were detected at MRA, and they had only one false-positive finding. The sensitivity and specificity were 97% and 100%, respectively. However, among the 64 aneurysms, seven (11%) could not be analyzed at TOF-MRA because of coil-related artifacts. A few patients were examined by means of contrast-enhanced MRA in this study; this approach

showed the advantage of contrast material injection in cases of large aneurysms. A more recent study (17) was performed to assess the interest in TOF-MRA with contrast material infusion in 68 patients. The results showed a sensitivity and a specificity of 72% and 98%, respectively. In our study, interobserver agreement in the detection of a residual aneurysmal neck was poor with TOF-MRA. This finding can be explained by the small size of the remnant necks and by the presence of flow-related artifacts that might have made analysis of MIP images difficult. Because of the better contrast of the source images, the use of the axial source images might have been helpful in interpreting MIP images, and the reliability of this technique might have been improved.

Important advances in MRA with contrast material injections allowed the use of a large imaging volume with a short acquisition time; high signal intensity in the vascular structures resulted from major shortening of the T1 in blood because of gadolinium-based contrast agent (18). Images are similar to those obtained at DSA; on these images, the signal intensity in the vascular lumen depends on the vascular concentration of gadolinium-based contrast agent at the time of image acquisition. This technique has proved its effectiveness in the evaluation of the cervical arteries (14). Few studies have been conducted to evaluate these sequences in imaging the circle of Willis (19–21), and to our knowledge, none have assessed the follow-up of patients who undergo GDC treatment for a ruptured aneurysm. This lack is probably explained by the presence of venous structures at the skull base and by the limited spatial resolution that may prevent its use in routine evaluation. In a recent study, Metens et al (16) evaluated this technique in 32 patients who were admitted to the hospital for a suspected intracranial aneurysm. Findings showed a high sensitivity and specificity of 100% and 96%, respectively. Only one false-positive finding was observed. TOF-MRA had a sensitivity and a specificity of 96% and 100%, respectively.

Potential advantages of using contrast-enhanced MRA in the detection and follow-up of intracranial aneurysms can be highlighted. First, the assessment of the first pass of a bolus of gadolinium-based contrast agent decreases the saturation or turbulence effects that are usually observed with TOF-MRA. This effect theoretically results in higher signal intensity in the residual aneurysmal sac, with images similar to those obtained with DSA. Second, the imaging volume may be orientated in the frontal plane, which allows us to assess a large volume from the intracranial segment of the vertebral arteries to the pericallosal portion of the anterior cerebral arteries. In contrast, the imaging volume of TOF-MRA must be orientated in the axial plane to optimize flow-related enhancement. Finally, the injection of contrast material allows better visualization of small vessels. This effect is because of the appropriate filling of small arteries with the gadolinium-based contrast agent and the short acquisition time of the sequence, which decreases the risk of motion artifacts (22).

In our study, the visualization of the anterior cerebral arteries was improved with the injection of contrast material. Coil artifacts seemed less apparent on contrast-enhanced MRA images compared with those on TOF-MRA images, and this difference is probably due to the shorter TE that decreases magnetic susceptibility artifacts (10, 12). However, the present study may have several shortcomings. The number of patients was limited, and only aneurysms of the AcomA were assessed. The particular anatomy of the AcomA probably accounts for the correct visualization of this artery on axial views and the absence of major venous overlap. Thus, our findings do not allow us to draw a conclusion about the reliability of this technique in the visualization of the other arterial segments in the circle of Willis.

Conclusion

Our findings showed the potential utility of contrast-enhanced MRA in the follow-up of patients treated with GDC for an aneurysm of the AcomA. The image quality was appropriate in all cases, with good agreement between DSA and MRA results in the detection of a residual neck. However, the limited spatial resolution of these sequences and the potential for venous enhancement after the injection of contrast material could limit the use of this technique in routine evaluation. These drawbacks will probably be overcome in the near future with the use of high-resolution ultrafast sequences.

References

1. Schievink WI. **Intracranial aneurysms.** *N Eng J Med* 1997;336: 28–40
2. Guglielmi G, Vinuela F, Dion J, Duckwiler G. **Electrothrombosis of saccular aneurysms via endovascular approach, I: preliminary clinical experience.** *J Neurosurg* 1991;75:8–14
3. Vinuela F, Duckwiler G, Mawad M, Guglielmi G. **Detachable coil embolization of acute intracranial aneurysm: perioperative anatomical and clinical outcome in 403 patients.** *J Neurosurg* 1997;86: 475–482
4. Korogi Y, Takahashi M, Katada K, et al. **Intracranial aneurysms: detection with three-dimensional CT angiography with volume rendering-comparison with conventional angiographic and surgical findings.** *Radiology* 1999;211:497–506
5. Ruggieri PM, Laub GA, Masaryk TJ, Modic MT. **Intracranial circulation: pulse-sequence considerations in three-dimensional MR angiography.** *Radiology* 1989;171:785–791
6. Ross JS, Masaryk TJ, Modic MT, Ruggieri PM, Haacke EM, Selman WR. **Intracranial aneurysms: evaluation by MR angiography.** *AJNR Am Neuroradiol* 1990;11:449–455
7. Huston J, Rufenacht DA, Ehamn RL, Wiebers DO. **Intracranial aneurysms and vascular malformations: comparison of time-of-flight and phase contrast MR angiography.** *Radiology* 1991;181:721–730
8. Edelman RR, Sungkee SA, Chien D. **Improved time-of-flight MR angiography of the brain with magnetization transfer contrast.** *Radiology* 1992;184:395–399
9. Derdeyn CP, Graves VB, Tursky PA, Masaryk AM, Strother CM. **MR angiography of saccular aneurysms after treatment with Guglielmi detachable coils: preliminary experience.** *AJNR Am Neuroradiol* 1997;18:279–286
10. Gönner F, Heid L, Remonda G, et al. **MR angiography with ultrashort echo time in cerebral aneurysms treated with Guglielmi detachable coils.** *AJNR Am J Neuroradiol* 1998;19:1324–1328
11. Kähära VJ, Seppänen SK, Ryymin PS, Mattila P, Kuurne T, Laasonen EM. **MR angiography with three-dimensional time-of-flight and targeted maximum-intensity-projection reconstructions in the follow-up of intracranial aneurysms embolized with Guglielmi de-**

tachable coils. *AJNR Am J Neuroradiol* 1999;20:1470–1475
12. Anzalone N, Righi C, Simionato F, Scomazzoni F, et al. **Three-dimensional time-of-flight MR angiography in the evaluation of intracranial aneurysms treated with Guglielmi detachable coils.** *AJNR Am J Neuroradiol* 2000;21:746–752
13. Jung HW, Chang KY, Choi DS, Han HM, Han CM. **Contrast-enhanced MR angiography for the diagnosis of intracranial vascular disease: optimal dose of gadopentetate dimeglumine.** *AJR Am J Roentgenol* 1995;165:1251–1255
14. Remonda L, Heid O, Schroth G. **Carotid artery stenosis, occlusion, and pseudo-occlusion: first pass gadolinium-enhanced three dimensional MR angiography-preliminary study.** *Radiology* 1998;209: 95–102
15. Jäger HR, Ellamushi H, Moore EA, Grieve JP, Kitchen ND, Taylor WJ. **Contrast-enhanced MR angiography of intracranial giant aneurysms.** *AJNR Am J Neuroradiol* 2000;21:1900–1907
16. Metens T, Rio F, Balériaux D, Roger T, David P, Rodesh G. **Intracranial aneurysms: detection with gadolinium-enhanced dynamic three-dimensional MR angiography-Initial results.** *Radiology* 2000;216:39–46
17. Boulin A, Pierot L. **Follow-up intracranial aneurysms treated with detachable coils: comparison of gadolinium enhanced 3D time-of-flight MR angiography and digital subtraction angiography.** *Radiology* 2001;219:108–113
18. Prince MR, Narasimham DL, Stanley JC, et al. **Breath-hold gadolinium-enhanced MR angiography of the abdominal aorta and its major branches.** *Radiology* 1995;197:785–792
19. Parker D, Tsuruda J, Goodrich C, Alexander A, Buswell H. **Contrast-enhanced magnetic resonance angiography of cerebral arteries.** *Invest Radiol* 1998;33:300–313
20. Talaga S, Jungreis CA, Kanal E. et al. **Fast Three-dimensional time-of-flight MR angiography of the intracranial vasculature.** *J Magn Reson Imag* 1995;5:317–323
21. Isoda H, Takehara Y, Isogai S et al. **Software-triggered contrast-enhanced three-dimensional MR angiography of the intracranial arteries.** *AJR Am J Roentgenol* 2000;174:371–375
22. Anthony MM, Frayne R, Unal O, Rappe AH, Strother CM. **Utility of CT angiography and MR angiography for the follow-up of experimental aneurysms treated with stents or Guglielmi detachable coils.** *AJNR Am J Neuroradiol* 2000;21:1523–1528